Wireless Personal Communications manuscript No.
(will be inserted by the editor)

A maximum likelihood UWB localization algorithm exploiting knowledge of the service area layout.

Eva Arias-de-Reyna · Umberto Mengali

the date of receipt and acceptance should be inserted later

Abstract In this paper a method for ultra-wideband (UWB) localization for indoor applications is proposed. Beacons at known locations exchange signals with a tag to the purpose of estimating its position from range measurements. These measurements are accurate only when the ray corresponding to the direct path (DP) from tag to beacon is strong enough. In an UWB indoor environment, however, the DP may be blocked by thick walls or metallic obstacles, giving rise to large range errors. Several methods are available to mitigate this problem, exploiting different degrees of prior information. Techniques exploiting range error models or based on traditional fingerprinting lead to better results than methods that do not require any prior knowledge.

This work has been supported by the Ministerio de Ciencia e Innovación (Spanish Government) through the Project CSD2008-00010 COMONSENS of the Consolider-Ingenio 2010 Program, by the Ministerio de Ciencia e Innovación (Spanish Government) and the European Union (FEDER) under grant TEC2009-14504-C02-02/TCM, and by Junta de Andalucía (TIC-155).

E. Arias-de-Reyna
Department of Signal Theory and Communications, University of Seville, Camino de los Descubrimientos s/n, 41092 Seville, Spain
Tel.: +34 95 448 21 77, Fax: +34 95 448 73 41
E-mail: earias@us.es

U. Mengali
Department of Information Engineering, University of Pisa, Via Caruso 16, 56122 Pisa, Italy
E-mail: umberto.mengali@iet.unipi.it

We propose a new method that combines the maximum likelihood principle with range error models and special fingerprints. Its performance, assessed by simulation and compared to other techniques, is shown to be superior to traditional fingerprinting in the presence of environmental changes.

Keywords UWB · localization · Undetected Direct Path · Time Of Arrival

1 Introduction

In the last few years wireless indoor geolocation has become an important technology for use in a variety of civil and military applications. In the commercial world, for example, there is an increasing need for identifying the position of specific items in warehouses and cargo ships, or for tracking people with special needs in residential environments, hospitals and nursing homes [1–3]. As recognized in the IEEE standard 802.15.4a [4], ultra-wideband (UWB) impulse radio can play a significant role in this context as it allows centimeter accuracy in ranging and low-power and low-cost communications.

In this paper we concentrate on indoor geolocation with UWB techniques. In particular we consider a network of beacons deployed inside a building and emitting UWB signals. Their location is known while the unknown coordinates of a tag must be determined from time-of-arrival (TOA) measurements. We envisage a scenario in which the tag position is restricted within a specific service area. For example we want to estimate the position of a robot as it moves inside a laboratory. For simplicity we concentrate on two-dimensional positioning.

Three beacons are sufficient to accurately solve the problem when direct paths (DPs) exist from tag to beacons and their strengths are sufficient to guarantee accurate TOA measurements [5]. However the DP may be obstructed or attenuated to such a degree that its energy falls below the detection threshold. This situation is called undetected direct path (UDP). When it happens, a ray arriving from a reflection can be erroneously declared as DP, so giving rise to a range estimate with a positive bias [2, 6]. It should be emphasized that the distinction between detected DP (DDP) and undetected DP does not correspond to the alternative line of sight (LOS) against non-LOS (NLOS) usually adopted in literature. Indeed LOS/NLOS refers to the presence/absence of a physical line of sight. On the other hand, DDP refers to the detectability of the direct path. Thus, DDP may be associated either to LOS or NLOS situations, as long as the energy of the direct ray reaches the detection threshold [2,7].

The simple least squares (LS) location estimator suffers severe degradations in UDP conditions [8, 9] and several strategies have been proposed to improve its performance. They exploit prior information that may be available in various forms: (*a*) knowledge on the range error statistics; (*b*) knowledge of the service area layout; (*c*) location fingerprints taken over the service area [1,10,11]. Point (*a*) refers to the probability density functions (PDFs) of the range errors at any given tag position under DDP or UDP conditions and to the prior probabilities of DDP/UDP occurrence. For example, mathematical models for the range errors in a typical UWB environment are given in [7,12,13]. Point (*b*) refers to the geometry of the service area (perimeter, inside walls, etc.) and to the presence of metallic objects in the building (elevator shafts, metallic doors, chambers etc.) that obstruct the direct connection between tag

and beacon. UDP mitigation strategies may be ranked according to the amount of prior information they exploit. The more information they use, the more efficient they are.

A simple UDP mitigation scheme is proposed in [14]. No information on the range error statistics is requested; only range measurements are used. The key idea is that, if the UDP measurements are relatively few, they can be identified and discarded (or downgraded). In this spirit the measurements from all the beacons are taken in combinations of three or more and, for each combination, an intermediate LS location estimate is computed. Its residual over the range measurements provides an indicator of the estimate reliability. A similar UDP mitigation scheme (but easier to implement) is discussed in [15].

In [16] the UDP measurements are viewed as data affected by gross errors, inconsistent with the range error distribution in DDP conditions. As such, they are regarded as *outliers*. Several robust algorithms exist that can cope with a certain percentage of outliers [17]. Among them the authors choose the *least median of squares* estimator.

In [18] a wideband CDMA cellular system is envisioned in which location measurements are based on time-difference-of-arrivals (TDOAs) and angle-of-arrivals (AOAs). While the scenario exhibits significant differences in error statistics compared with an indoor UWB environment, the methods in [18] can be extended to the problem discussed in the present paper.

Reference [19] investigates a localization algorithm that assumes knowledge of the floor plan. This allows one to establish how many walls are crossed by a given tag-to-beacon path and, in consequence, the ranging error resulting from excess de-

lay due to intra-wall propagation. Subtracting this error from the range measurement provides a more accurate estimate of the tag-to-beacon distance. Only DDP conditions are considered since no metallic obstructions are envisioned in the service area. The algorithm proceeds in two steps. In the first one a rough tag location estimate is produced by application of the LS method, without exploiting the floor plan knowledge. Next, assuming that the estimate is accurate, the ranging errors due to excess delay are compensated for in the range measurements and a new application of the LS method produces the final location estimate.

Mapping methods referred to as *location fingerprinting* [1, 11, 20] offer another way to counteract UDP conditions. Assuming that the service area is relatively small, the idea is to perform pre-measurements at each possible tag position and to compile a database of range signatures. Each signature consists of a vector providing the measured distances from tag to beacons. A nearest-neighbor algorithm determines the signature in the database with the minimum Euclidean distance to the actual range metrics. Fingerprinting methods are usually very accurate but are not robust against environmental changes due to moving obstacles [1]. Such changes produce a mismatch between recorded and online measurements and call for database updates which are expensive and time consuming.

In the present paper we discuss a maximum likelihood (ML) position estimator that makes use of an alternative fingerprinting technique in which signatures tell us tag-to-beacon DDP/UDP conditions rather than tag-to-beacon ranges. In particular, the nth signature component is either zero or one, depending on whether the DP from the nth beacon can be detected or not. Bearing in mind that UWB signals penetrate

walls of reasonable thickness while they are blocked by metallic reflectors [2, 7], it follows that DDP/UDP signatures can be extracted from: (*a*) the infrastructure of the service area, taking into account size and position of the major metallic objects; (*b*) field measurements when necessary.

The advantage of DDP/UDP signatures over range signatures consists in a greater robustness against environmental changes. For example, suppose that the DP from the *n*th beacon is blocked by a metallic chamber, so creating a shadow zone where the tag is only reached through indirect paths. Also, assume that some people are moving around the chamber. As long as the tag lies in the shadow zone, the *n*th component of a DDP/UDP signature is unity, independently of the presence of people. On the contrary, in a range signature it may vary, depending on the positions of the people.

The main contributions of this paper are:

- Use of the DDP/UDP signature to represent the propagation conditions at a given tag position.
- Performance comparisons between the ML position estimator and other localization methods available in literature.
- Assessment of the robustness of all these methods against environmental changes.

The rest of the paper proceeds as follows. In Section II a specific service area is taken as a study case to assess the performance of localization methods. As we shall see, the DDP/UDP database is easily computed from the floor plan. Similarly, the range database and the PDFs of the range errors are derived from a statistical model of the range measurements. Section III describes the ML position estimator while

Section IV overviews the operation of the other positioning schemes. Section V provides simulation results and comparisons while Section VI offers some conclusions.

2 Study case

2.1 Floor plan

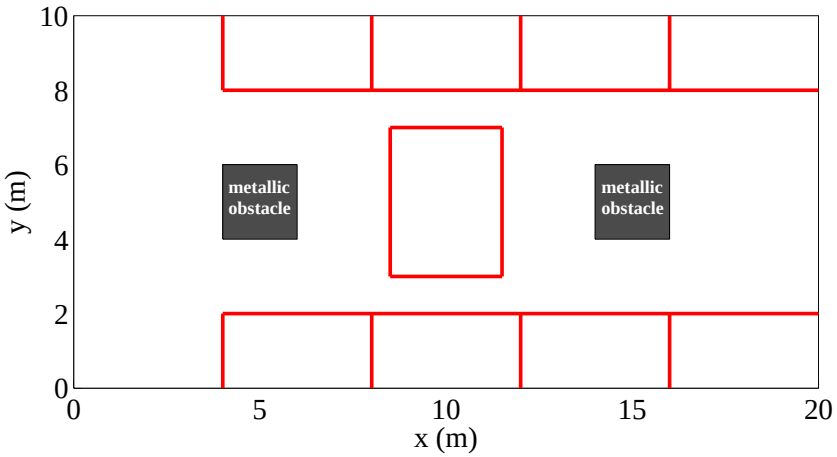

Fig. 1 Floor plan taken as a study case

Figure 1 shows the floor plan taken as a study case. It consists in a rectangular area of size 20 m $\times$ 10 m, with two internal square metallic objects, each of side 2 m, and a number of nonmetallic panels. The metallic objects completely block the UWB signals and generate shadow zones with UDP conditions. The panels are approximated to be thin and transparent to signals. A ray impinging on a panel is split

into a transmitted and a reflected ray. The former proceeds along the extension of the incident ray while the latter goes in a new direction that depends on the orientation of the panel. Figure 2 depicts the UDP zones for a beacon lying in the lower corner on the left hand side. For any tag position the DDP/UDP signature is computed setting its nth component to 1 or 0 depending on whether the tag is or is not in the UDP zone of the nth beacon. The collection of the DDP/UDP signatures taken over all the possible tag positions produces the DDP/UDP database. The set of possible tag locations is considered to be the set of nodes of a grid covering the floor plan, excluding the sub-areas the tag cannot reach. In the simulations reported later a mesh size of 10 cm has been chosen.

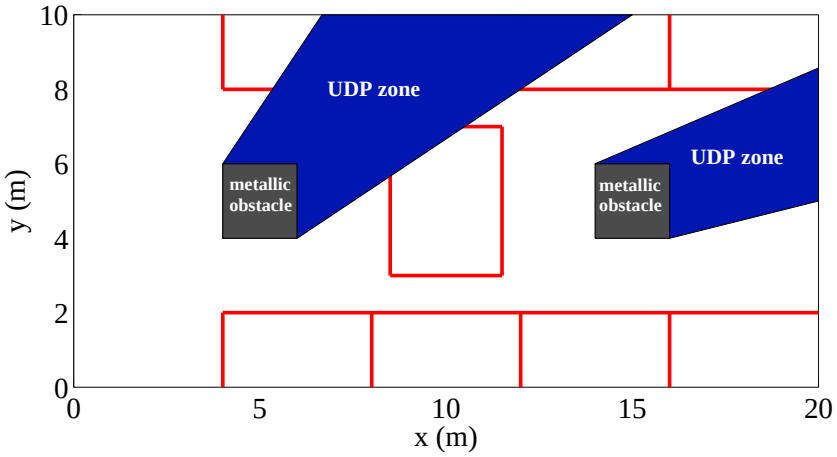

Fig. 2 Service area and UDP zones for a beacon lying at (0,0)

This scenario is readily extended to the case in which the UDP conditions are caused by a large distance from tag to beacon, such that the DP is attenuated below the detection threshold [7].

2.2 Models for range measurements

References [7, 12] discuss statistical models for range measurements taken in indoor UWB environments. In this section we draw from [12] to construct analogous models for the specific floor plan in Fig. 1. To begin with, let us call $z = (x,y)^T$ the tag coordinates and $z_n = (x_n, y_n)^T$ ($n = 1,2,\cdots,N$) the coordinates of the nth beacon. We first assume DDP propagation conditions. Accordingly the range measurement may be written as

$$r_n = d_n + \varepsilon_{n,DDP} \tag{1}$$

where d_n is the line-of-sight (LOS) distance from tag to beacon

$$d_n = \sqrt{(x-x_n)^2 + (y-y_n)^2} \tag{2}$$

while $\varepsilon_{n,DDP}$ is the range error. As explained in [7, 12], $\varepsilon_{n,DDP}$ results from the presence of propagation paths close to the DP. These paths perturb the channel response around the DP peak and produce a shift in the apparent DP arrival time. The shift depends on the number, amplitude and phase of those paths and on the system bandwidth. The narrower the bandwidth, the larger the errors. Experimental results in [12]

suggest the following expression of $\varepsilon_{n,DDP}$

$$\varepsilon_{n,DDP} = \gamma \log(1 + d_n) \tag{3}$$

where d_n is in meters and γ is a Gaussian random variable with mean m_γ and standard deviation σ_γ. The dependence of $\varepsilon_{n,DDP}$ on d_n is in keeping with our intuition that the errors increase with the distance from transmitter to receiver. For a system bandwidth of 500 MHz, as is assumed henceforth, reference [12] provides the empirical values m_γ=21 cm and σ_γ=26.9 cm.

It follows from (3) that $\varepsilon_{n,DDP}$ is Gaussian with mean

$$m_{n,DDP} = m_\gamma \log(1 + d_n) \tag{4}$$

and standard deviation

$$\sigma_{n,DDP} = \sigma_\gamma \log(1 + d_n) \tag{5}$$

Thus, the PDF of r_n takes the form

$$p_{DDP}(r_n; z) = \frac{1}{\sqrt{2\pi}\sigma_{n,DDP}} \exp\left[-\frac{(r_n - d_n - m_{n,DDP})^2}{2\sigma_{n,DDP}^2} \right] \tag{6}$$

Next we turn our attention to UDP propagation conditions. As the DP is undetected, the shortest path from tag to beacon has a length $d_n^{(s)}$ greater than d_n. Thus, paralleling the arguments leading to (1) and (3) we get

$$r_n = d_n^{(s)} + \varepsilon_{n,UDP} \tag{7}$$

with

$$\varepsilon_{n,UDP} = \gamma \log(1 + d_n^{(s)}) \tag{8}$$

where γ is as in (3). It follows that $\varepsilon_{n,UDP}$ is Gaussian with mean

$$m_{n,UDP} = m_\gamma \log(1 + d_n^{(s)}) \tag{9}$$

and standard deviation

$$\sigma_{n,UDP} = \sigma_\gamma \log(1 + d_n^{(s)}) \tag{10}$$

The difference between (1) and (7) is worth noting. While in (1) the LOS distance d_n is easily derived from (2), in (7) the shortest path length $d_n^{(s)}$ needs to be computed with a ray tracing algorithm. In the simulations reported later we used such an algorithm to generate the set $\{d_n^{(s)}\}$ for $n = 1, 2, ..., N$ and z varying over the nodes of the grid covering the floor plan in Fig. 1.

Fig. 3 illustrates the connections to beacons for a tag situated at $(6.5, 4.5)$ m, in the case of four beacons at the corners of the service area. Beacons 2 and 3 are in DDP connection with the tag, thus the ray trajectories coincide with the direct paths in these cases, represented with dashed lines. On the contrary, beacons 1 and 4 are in UDP condition with respect to the tag because a large metallic object blocks the direct path, thus the shortest paths (dash-dotted lines), computed with a ray tracing algorithm, involve reflections and are longer than the direct paths.

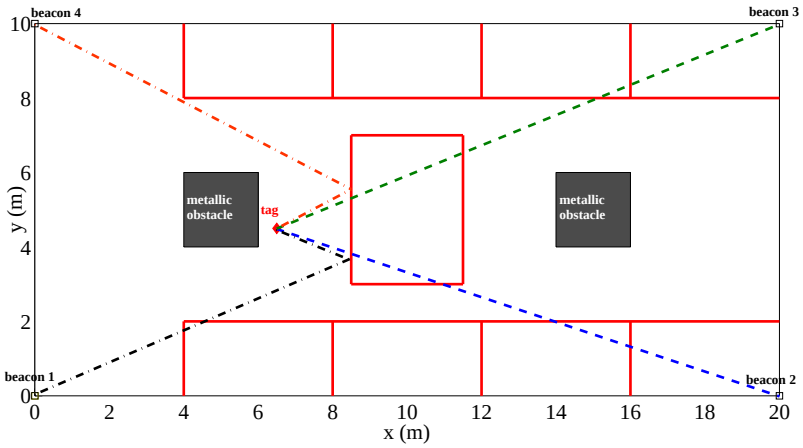

Fig. 3 Trajectories corresponding to the shortest tag-beacon paths, for a tag situated at $(6.5,4.5)m$ in the floor plan of Fig. 1, with four beacons.

2.3 Range database generation

Range measurements can be simulated at any tag position and for any beacon by generating Gaussian random variables according to (1) or (7). Collecting the measurements at a given z produces a range signature while collecting the signatures as z visits all the nodes of the grid produces the range database.

For example, suppose there are three beacons: the first in the bottom corner on the left in Fig. 2, the second in the bottom corner on the right, and the third in the upper corner on the right. Table 1 gives the portion of the generated database corresponding to the z-positions for $x = 16.5m$, between $y = 3m$ and $y = 5m$, at a distance of 10 cm from each other. Parameters m_γ and σ_γ are set to 21 cm and 26.9 cm, respectively.

The table is organized in three columns. The first gives the running index $n = 0,1,\cdots,20$ for the considered portion of the database. The second gives the coordinates of the tag position $(16.5,3+0.1n)$ in meters. The third gives the corresponding

n	$(x,y)[m]$	$(r_1,r_2,r_3)[m]$
0	(16.5,3)	(17.71,5.22,8.17)
1	(16.5,3.1)	(17.75,5.08,7.93)
2	(16.5,3.2)	(16.94,5.21,8.49)
3	(16.5,3.3)	(17.31,5.62,8.00)
4	(16.5,3.4)	(17.31,5.19,7.84)
5	(16.5,3.5)	(18.04,5.60,7.77)
6	(16.5,3.6)	(17.70,5.48,7.75)
7	(16.5,3.7)	(17.89,5.55,7.63)
8	(16.5,3.8)	(17.33,5.62,7.65)
9	(16.5,3.9)	(17.59,5.53,7.14)
10	(16.5,4.0)	(17.20,5.90,7.56)
11	(16.5,4.1)	(17.60,5.81,7.44)
12	(16.5,4.2)	(18.95,5.47,7.93)
13	(16.5,4.3)	(20.55,5.92,7.02)
14	(16.5,4.4)	(23.89,5.62,6.72)
15	(16.5,4.5)	(24.20,6.13,6.69)
16	(16.5,4.6)	(24.58,6.55,6.50)
17	(16.5,4.7)	(23.94,6.13,7.02)
18	(16.5,4.8)	(24.54,5.90,6.44)
19	(16.5,4.9)	(24.26,6.51,6.95)
20	(16.5,5.0)	(24.88,6.75,6.50)

Table 1 Portion of the generated database corresponding to the z-positions for $x = 16.5m$, between $y = 3m$ and $y = 5m$

generated signature (r_1,r_2,r_3). As n varies, the tag is always in DDP connection with beacons 2 and 3 while it falls into the UDP zone of beacon 1 for $n > 12$. These facts are reflected in the behavior of the signature components. Indeed, as the tag moves away from beacon 2 and gets closer to beacon 3, r_2 tends to increase while r_3 tends to decrease. Meanwhile r_1 appears to be almost constant till $n = 12$ (the true distance increases very slowly but this increase is concealed by the additive random measurement error) and then exhibits a jump when the tag enters the UDP zone.

3 ML location estimator

In this section we propose an ML location estimator that exploits both the DDP/UDP database and statistical information on the range measurements, as expressed by the conditional PDFs of r_n under DDP and UDP.

For the PDF conditioned on DDP we choose (6). Parameters m_γ and σ_γ appearing in (4)–(5) are computed from the range database as follows. For each beacon the subset of tag locations corresponding to DDP is considered and for each location the corresponding r_n is picked up from the range database. This provides a realization of the range error $\varepsilon_{n,DDP} = r_n - d_n$ as well as of γ (making use of (3))

$$\gamma = \frac{r_n - d_n}{\log(1+d_n)} \tag{11}$$

from which m_γ and σ_γ are derived in a straightforward way taking averages over the DDP locations and the N beacons.

In the UDP case, instead, we deviate from (7) because of the computational complexity involved in getting $d_n^{(s)}$. Looking for a simpler route, we rewrite (7) as the sum of d_n (not $d_n^{(s)}$) plus a deviation $\tilde{\varepsilon}_{n,UDP}$

$$r_n = d_n + \tilde{\varepsilon}_{n,UDP}. \tag{12}$$

Next we assume that $\tilde{\varepsilon}_{n,UDP}$ is Gaussian and approximately independent of the beacon index n and the tag position z. Accordingly we write $\tilde{\varepsilon}_{UDP}$ instead of $\tilde{\varepsilon}_{n,UDP}$. Note that this Gaussian model may not accurately reflect the experimental reality. Actually we take it just for mathematical convenience as it paves the floor to a simple

expression of the PDF of r_n. Its effectiveness will be judged from the performance of the resulting ML location estimator. In conclusion, the PDF of r_n becomes

$$p_{UDP}(r_n;z) = \frac{1}{\sqrt{2\pi}\tilde{\sigma}_{UDP}} \exp\left[-\frac{(r_n - d_n - \tilde{m}_{UDP})^2}{2\tilde{\sigma}_{UDP}^2}\right] \tag{13}$$

We are left with the problem of assigning sensible values to $\tilde{m}_{UDP}$ and $\tilde{\sigma}_{UDP}$. These parameters can be computed making use of the range database which, as indicated in Section II-C, can be generated once m_γ and σ_γ are established. The computation of $\tilde{m}_{UDP}$ and $\tilde{\sigma}_{UDP}$ proceeds as follows. For any pair (n,z) corresponding to UDP condition, the range database gives r_n. Also, as shown in (12), the difference $r_n - d_n$ gives $\tilde{\varepsilon}_{n,UDP}$. Thus, taking the arithmetic mean of $r_n - d_n$ over all the pairs (n,z) produces $\tilde{m}_{UDP}$. In the same way, taking the arithmetic mean of $(r_n - d_n)^2$ and subtracting $\tilde{m}_{UDP}^2$ provides $\tilde{\sigma}_{UDP}^2$. Note that while parameters $m_{n,DDP}$ and $\sigma_{n,DDP}$ in (6) depend on the pair (n,z), parameters $\tilde{m}_{UDP}$ and $\tilde{\sigma}_{UDP}$ in (13) are independent of both n and z. For example, assuming eight beacons deployed in the mid-points of the walls and the corners of the rectangular area in Fig. 1, it is found $\tilde{m}_{UDP}$=2.16 m and $\tilde{\sigma}_{UDP}$=1.76 m.

Proceeding with the derivation of the ML location estimator we divide the beacon indices at a given tag location into two subsets: one corresponding to DDP, say $\mathscr{I}_{DDP}(z)$, and the other corresponding to UDP, say $\mathscr{I}_{UDP}(z)$. Such a division is readily done by making use of the DDP/UDP database. Then, letting $r \triangleq (r_1, r_2, \cdots, r_N)^T$ and assuming the range measurements as statistically independent, the PDF of r reads

$$p(r;z) = \prod_{n\in\mathscr{I}_{DDP}(z)} p_{DDP}(r_n;z) \times \prod_{n\in\mathscr{I}_{UDP}(z)} p_{UDP}(r_n;z) \tag{14}$$

from which the log-likelihood function $\Lambda(r;z) \triangleq \ln p(r;z)$ is computed (within an irrelevant additive constant independent of z) as

$$\begin{aligned}\Lambda(r;z) = &- \sum_{n\in\mathscr{I}_{DDP}(z)} \ln\sigma_{n,DDP} \\ &- \sum_{n\in\mathscr{I}_{DDP}(z)} \frac{(r_n - d_n - m_{n,DDP})^2}{2\sigma^2_{n,DDP}} \\ &- \sum_{n\in\mathscr{I}_{UDP}(z)} \frac{(r_n - d_n - \tilde{m}_{UDP})^2}{2\tilde{\sigma}^2_{UDP}} \\ &- \sum_{n\in\mathscr{I}_{UDP}(z)} \ln\tilde{\sigma}_{UDP}\end{aligned} \tag{15}$$

The ML estimator looks for the maximum of $\Lambda(r;z)$ over all the possible tag locations z. Note that the maximization must be performed for z varying over the floor plan. In particular, the maximum of $\Lambda(r;z)$ is sought within the perimeter of the service area and outside the metallic obstacles.

4 Other positioning schemes

We now overview other localization methods to be compared with the ML algorithm.

4.1 Method in [14]

All the possible combinations of three or more range measurements are considered. Each combination is represented by the set of indices S_k $(k = 1,2,\cdots,K)$ of the corresponding beacons. For each set an intermediate LS estimate of z, $\hat{z}_k$, is computed by minimizing the quantity

$$\mathrm{Res}(z;S_k) = \sum_{n\in S_k} [r_n - \|z - z_n\|]^2 \tag{16}$$

The inverse of the normalized quantity $\Re(\hat{z}_k;S_k) \triangleq \frac{\mathrm{Res}(\hat{z}_k;S_k)}{\mathrm{Size\ of}\ S_k}$ is viewed as a measure of the reliability of the estimate $\hat{z}_k$ and the final estimate of z is taken as

$$\hat{z} = \frac{\sum_{k=1}^{K} \hat{z}_k (\Re(\hat{z}_k;S_k))^{-1}}{\sum_{k=1}^{K} (\Re(\hat{z}_k;S_k))^{-1}} \tag{17}$$

4.2 Method in [16]

The method in [16] is similar to that in [14], except that only combinations of three beacons at a time are considered and, instead of minimizing the *sum* of the squared residues, the *median* of the residues is minimized.

4.3 Method in [18]

The method in [18] does not exploit any DDP/UDP database. Indeed propagation conditions are expressed in statistical form, calling $P_n^{(DDP)}(z)$ the probability that there is a DDP from tag to the nth beacon, and $P_n^{(UDP)}(z)$ the complementary probability that the DP is undetected. Then, the likelihood function becomes

$$p(r;z) = \prod_{n=1}^{N} \Big[\, p_{DDP}(r_n;z)\, P_n^{(DDP)}(z) + p_{UDP}(r_n;z)\, P_n^{(UDP)}(z) \Big] \tag{18}$$

The authors in [18] look for the maximum of a modified version of (18) in which $P_n^{(DDP)}(z)$ and $P_n^{(UDP)}(z)$ are replaced by quantities $P_n^{(DDP)}$ and $P_n^{(UDP)}$ independent of z. One difficulty in going on is to assign sensible values to those quantities. We

explored two routes. In one case we put $P_n^{(DDP)}$ equal to the fraction of the service area in LOS connection with the nth beacon. In the other we set $P_n^{(DDP)} = P_n^{(UDP)} = 1/2$, which corresponds to having no idea about the link propagation conditions. As experimental evidence shows minimal difference in the results, in the following we only report on the second case.

4.4 Range-based fingerprinting

Range-based fingerprinting works in two stages: offline and online stage. The former consists in taking range fingerprints as a function of the tag position all over the service area. As a result the database is generated. During the latter stage a fingerprint is measured at the unknown tag location and an algorithm is used to identify the recorded fingerprint closest to the measured one. In order to improve performance, the fingerprint for each location may be obtained as the average of a few offline independent measurements. In the simulations reported below, we took the average of four independent measurements.

5 Simulation results

Simulations have been run relative to the specific service area of Section 3. The signature database is generated as explained in section 2.3. A total of 2000 random tag locations are considered and, for each location, 10 different realizations of the range measurements are generated, leading to a total of 20000 simulation trials. The ML estimator in Section 3 (henceforth referred to as MLE) is compared with the algorithms in [14, 16, 18] and the classical fingerprinting technique (CFT).

Letting $\hat{z}$ be the estimate of the tag position provided by a given algorithm, the estimation performance is expressed as the root mean square error (RMSE), which is defined as the square root of the average of $\|z-\hat{z}\|^2$ taken over z. The number of beacons N varies from 3 to 8. The first two are placed in the corners on the bottom. The 3rd one is in the upper corner on the right. The 4th lies in the remaining corner. The 5th and 6th are set at the mid points of the longer walls while the 7th and 8th lie in the mid points of the shorter walls.

All the algorithms exploit knowledge of the floor plan in the sense that locations outside the perimeter or inside the metallic obstacles in the service area are excluded.

Figure 4 makes comparisons and illustrates the tradeoff between prior information (in the form of range error models or actual offline range measurements) and localization accuracy. As expected, the CFT has the best performance as it exploits all the information from the range database. The MLE is somewhat inferior, only for a small number of beacons. Intuitively this is so because it has no direct access to the range database. Its functioning relies in part on the DDP/UDP database (which is less informative than the range database) and in part on averaging operations on the fingerprints of a range database obtained from a single offline measurement for each tag location. The third best algorithm is that in [18] which, as opposed to MLE, does not exploit the DDP/UDP database. Last come the algorithms in [14] and [16] which have no information on channel statistics.

It is interesting to see what happens if the environment is changed. We consider two possible modifications of the floor plan. One consists in adding a number of non-metallic obstacles (as illustrated in Fig. 5) and the second in removing some of the

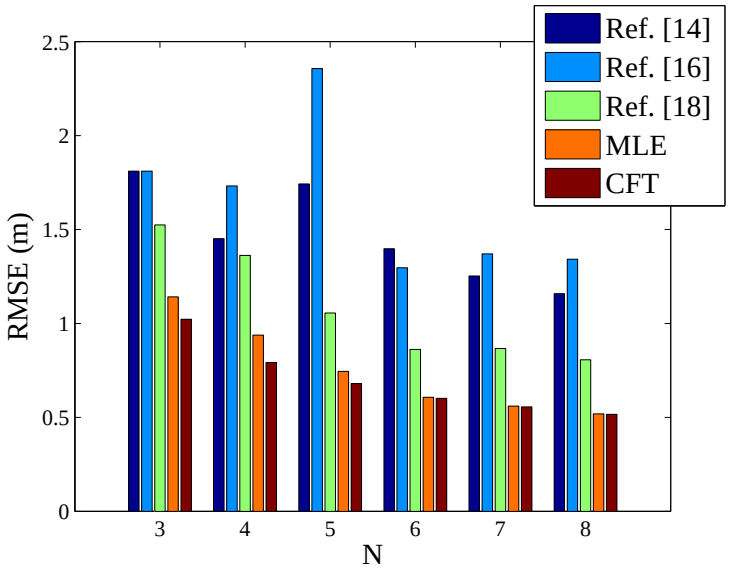

Fig. 4 RMSE of the positioning error for different localization techniques as a function of the number of beacons, for the floor plan in Fig. 1

panels (as shown in Fig. 6). The localization algorithms are tested without updating their prior information on the floor plan. In other words, they wrongly believe that the plan is still as shown in Fig. 1, which implies that the range database and the conditional PDF $p_{UDP}(r_n;z)$ are the same[1] as in Fig. 4. Figures 7 and 8 show the results. We see that the performance of CFT is considerably degraded, while the behavior of MLE is virtually unaltered. With the only exception of the case $N = 3$ of Fig. 8, the MLE is now superior to any other localization method.

[1] As the panels and the added obstacles let the signals pass through, the DDP/UDP database and $p_{DDP}(r_n;z)$ do not change as the panels are moved.

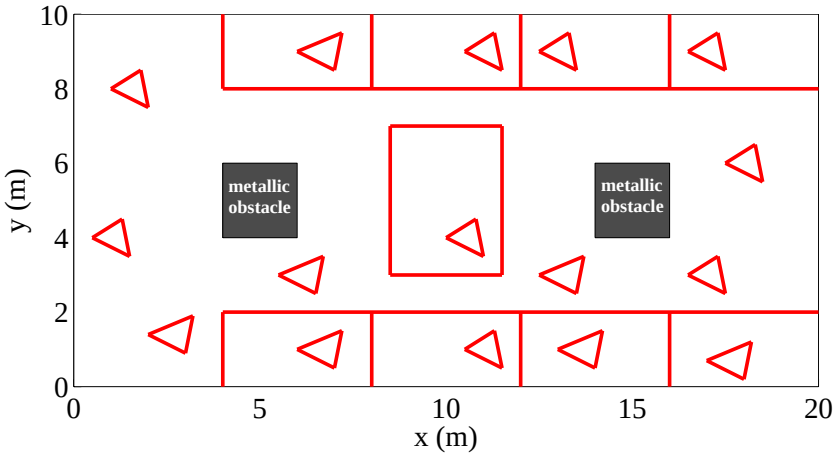

Fig. 5 Floor plan resulting from adding some non-metallic obstacles to the scenario of Fig. 1

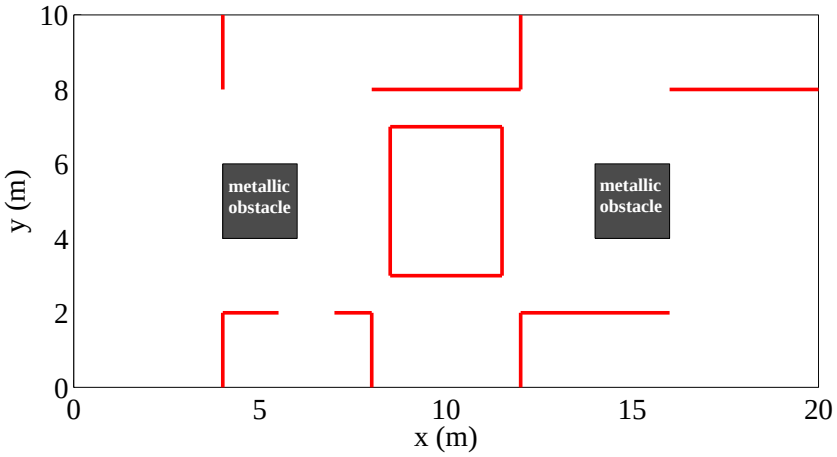

Fig. 6 Floor plan resulting from removing some panels from the scenario of Fig. 1

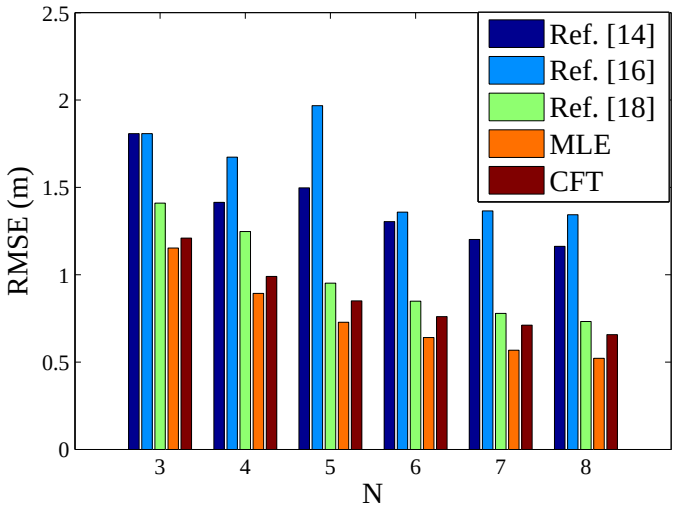

Fig. 7 RMSE of the positioning error for different localization techniques as a function of the number of beacons, for the floor plan in Fig. 5

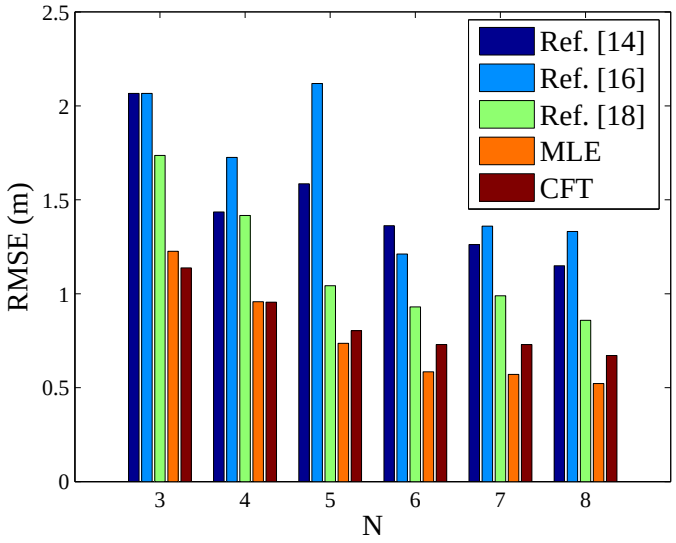

Fig. 8 RMSE of the positioning error for different localization techniques as a function of the number of beacons, for the floor plan in Fig. 6

6 Conclusions

We have proposed an ML positioning method that exploits an UDP/DDP database along with range error statistics. The UDP/DDP database is simpler to implement than the range database adopted in the classical range-based fingerprinting technique. In order to assess the performance of the proposed algorithm, we have also presented a comparative study on a variety of TOA-based geolocation algorithms for UWB indoor applications. The conclusions of this study are as follows.

As expected, a tradeoff exists between performance and complexity of the algorithms. The simplest localization methods do not use information on the range error statistics and the environment layout but exhibit the worst performance. The proposed ML algorithm is more complex but is definitely superior. The classical fingerprinting technique is even better as long as the scenario for which the range database was generated remains unchanged. Significant degradations occur, however, if environmental changes are not accounted for. This is in contrast with the behavior of the proposed ML method which is robust against modifications in the floor plan.

References

1. K. Pahlavan and X. Li. Indoor geolocation science and technology. *IEEE Communications Magazine*, 40(2):112–118, February 2002.
2. K. Pahlavan, F. O. Akgul, M. Heidari, and A. Hatami. Indoor geolocation in the absence of direct path. *IEEE Wireless Communications*, 13(6):50–58, December 2006.
3. S. Gezici, Z. Tian, G. B. Giannakis, H. Kobayashi, A. F. Molish, H. V. Poor, and Z. Sahinoglu. Localization via ultra-wideband radios. *IEEE Signal Processing Magazine*, 22(4):70–84, July 2005.

4. IEEE Standard 802.15.4a-2007 Task Group. Part 15.4: Wireless medium access control (MAC) and physical layer (PHY) specifications for low-rate wireless personal area networks (WPANs). Technical report, March 2007.
5. A. H. Sayed, A. Tarighat, and N. Khajehnouri. Network-based wireless location. *IEEE Signal Processing Magazine*, 25:24–40, July 2005.
6. J-Y. Lee and R. A. Scholtz. Ranging in a dense multipath environment using an UWB radio link. *IEEE Transactions on Selected Areas in Communications*, 20(9):1677–1683, December 2002.
7. M. Heidari and K. Pahlavan. A new error statistical model for the behavior of ranging errors in TOA-based indoor localization. In *Proc. IEEE WCNC*, pages 2566–2571, 2007.
8. Y. Qi, H. Kobayashi, and H. Suda. On time-of-arrival positioning in a multipath environment. *IEEE Transactions on Vehicular Technology*, 55(5):1516–1526, September 2006.
9. Y. Qi, H. Kobayashi, and H. Suda. Analysis of wireless geolocation in a non-line-of-sight environment. *IEEE Transactions on Wireless Communications*, 5(3):672–681, March 2006.
10. P. Bahl and V. N. Padmanabhan. RADAR: An in-building RF-based user location and tracking system. In *Proc. IEEE INFOCOM*, volume 2, pages 775–784, Tel Aviv, Israel, 2000.
11. C. Steiner and A.. Wittneben. Low complexity location fingerprinting with generalized UWB energy detection receivers. *IEEE Transactions on Signal Processing*, 58(3):1756–1767, March 2010.
12. B. Alavi and K. Pahlavan. Modeling of the TOA-based distance measurements error using UWB indoor radio measurements. *IEEE Communications Letters*, 10(4):275–277, April 2006.
13. D. B. Jourdan, D. Dardari, and M. Z. Win. Position error bound for UWB localization in dense cluttered environments. In *Proc. International Conference on Communications, ICC 2006*, volume 8, pages 3705–3710, June 2006.
14. P-C. Chen. A non-line-of-sight error mitigation algorithm in location estimation. In *Proc. IEEE Wireless Communications and Networking Conference*, pages 316–320, New Orleans, September 1999.
15. X. Li. An iterative NLOS mitigation algorithm for location estimation in sensor networks. In *Proc. International Mobile and Wireless Communications Summit*, Myconos, Greece, 2006.
16. R. Casas, A. Marco, J. J. Guerrero, and J. Falco. Robust estimator for non-line-of-sight error mitigation in indoor localization. *EURASIP Journal on Applied Signal Processing*, pages 1–8, 2006.
17. P. J. Rousseeuv and A. M. Lery. *Robust regression and outlier detection*. John Wiley and Sons, Inc., Hoboken, New Jersey, 2003.

18. L. Cong and W. Zhuang. Nonline-of-sight error mitigation in mobile location. *IEEE Transactions on Wireless Communications*, 4(2):560–573, March 2005.

19. D. Dardari, A. Conti, J. Lien, and M. Z. Win. The effect of cooperation on localization systems using UWB experimental data. *EURASIP Journal on Advances in Signal Processing*, pages 1–11, 2008.

20. M. McGuire, K. N. Plataniotis, and A. N. Venetsanopoulos. Location of mobile terminals using time measurements and survey points. *IEEE Transactions on Vehicular Technology*, 52(4):999–1011, July 2003.

BIOGRAPHY OF E. ARIAS-DE-REYNA

Eva Arias-de-Reyna received the degree in Telecommunication Engineering and the Ph.D. degree from the University of Seville, Spain, in 2001 and 2007, respectively. Since 2002, after working in the industry for a year, she has been with the Department of Signal Theory and Communications at the University of Seville, where she is now an assistant professor (*Profesora Contratada Doctora*). Her current research interests include digital communications and localization techniques, with emphasis on Ultra Wideband (UWB) technology.

author's picture & biography
Click here to download author's picture & biography: Mengali_s Bio Sketch .eps

BIOGRAPHY OF U. MENGALI

Umberto Mengali received his education in Electrical Engineering from the University of Pisa. From 1963 to 2008 he has been with the Department of Information Engineering of the University of Pisa. In 2009 he has been appointed Professor Emeritus. He has served in a number of technical program committees of international conferences and has been technical Co-Chair of the 2004 International Symposium on Information Theory and Applications (ISITA). His research interests are in the area of digital communications and ultrawide bandwidth systems. He has co-authored the book “Synchronization Techniques for Digital Receivers” (Plenum Press, 1997). Professor Mengali is an IEEE Life Fellow and is a member of the IEEE Communication Theory Committee. He has been an editor of the IEEE Transactions on Communications and of the European Transactions on Telecommunications.